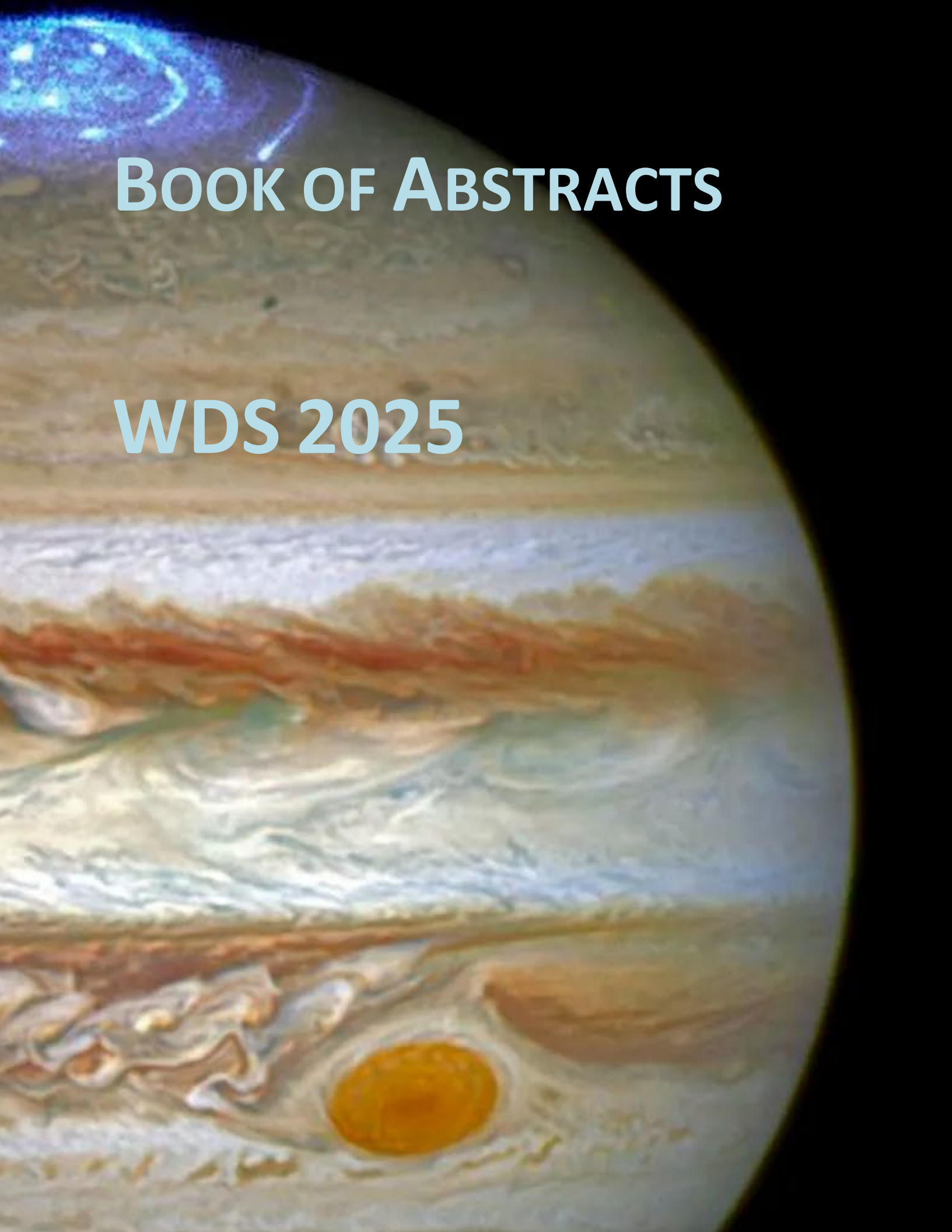

Book of Abstracts

WDS 2025

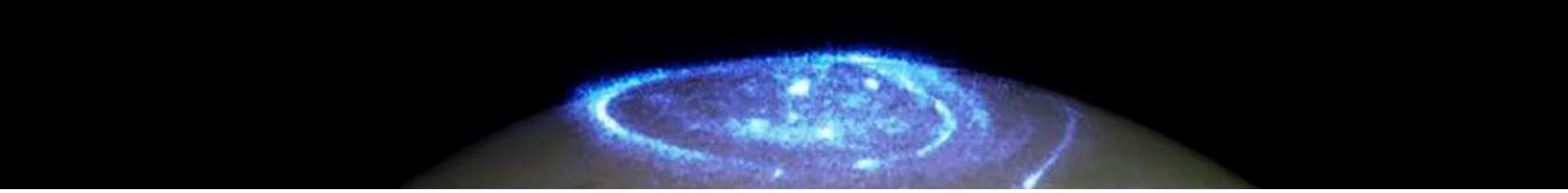

BOOK OF ABSTRACTS

Week of Doctoral Students 2025

Prague, June 3–5, 2025

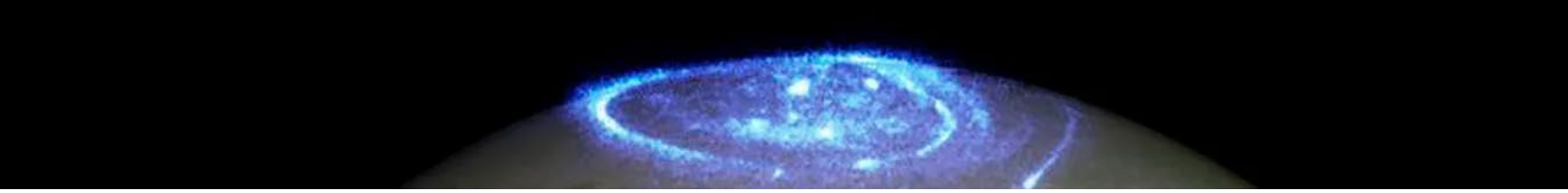

CONTENTS

Abstracts are listed alphabetically
by presenting authors in each section.

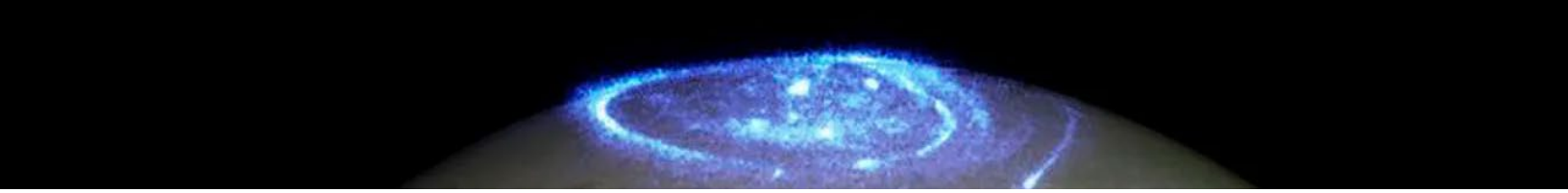

F-1 Theoretical Physics, Astronomy and Astrophysics

Covariant Phase Space and Homotopy Algebra

Bernardes V., Erler T., and Firat A. H.

Abstract. The covariant phase space formalism provides a framework for defining the symplectic form in field theories but is typically restricted to actions with finitely many spacetime derivatives. We address this limitation by constructing the symplectic form using the homotopy algebra approach to field theory. This enables a Hamiltonian formulation for arbitrary gauge theories, including non-local theories such as string field theory.

Quantum Phase Transitions and Nonlinear Dynamics in Cooled Ion Systems

Cepil A.

Abstract. Both the single-ion generalized Rabi model or multi-ion Dicke model for entangled linear Coulomb crystal suggest quantum phase transition (QPT) will occur under specific laser parameters at calcium clock transition frequency. This state is predicted to increase optical clock stability by reducing quantum projection noise. Theoretical models for the state preparation and probing have been used to design a laser sequence for the experimental realization of the QPT.

Gravitational Lensing from Stellar Remnants in the Galactic Center

Černý D. and Haas J.

Abstract. Although the number of predicted stellar black holes in the Galactic Center is in thousands, we cannot observe them directly. Therefore, we are exploring new ways of detecting them and their influence on stellar population, mainly gravitational lensing. We performed several N-body simulations of the Galactic Center with black holes and stars. There we looked for lensing events that lighten up the stars thus revealing the existence of a black hole in the Galactic center in future observations.

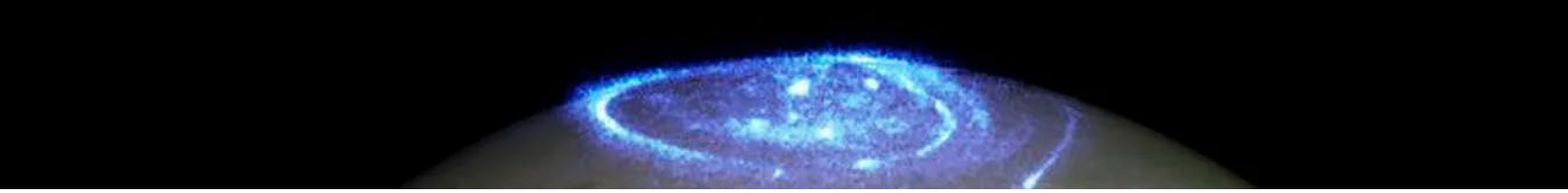

Quiver Sigma Model for Multi-center Black Hole

Raeymaekers J., Sanli C., Sengor G., Rossi P., and De Marco A.

Abstract. Quiver quantum mechanics describes bound states of D-branes as point particles in 3+1 dimensions with electric and magnetic charges, or centers, coupled to fermions. Coulomb quiver sigma models encode these charged centers as coordinates on a conical target space. In the scaling limit, centers approach the bottom of an AdS2 throat, capturing black hole microstates. We derive the conical metric explicitly for the 3-center case, with the aim to generalize it to the N-centers case.

Photometric Method Comparison and Short-term Variability Analysis of TESS Blazars with QPO Detection

Dzygunenko A., Baransky A., and Ridden-Harper R.

Abstract. We analyzed short-term optical variability in 16 TESS blazars using three extraction methods: Quaver and TESSreduce (PSF/Aperture). Quaver yielded the most consistent metrics (chi-square ≈ 70.2, excess variance ≈ 1.67, RMS ≈ 9.49). PSF produced sharper curves but sometimes unreliable results; Aperture showed high noise. QPOs (0.7–11 d) were detected from Quaver using WWZ and LSP. Deviations from Gaussian flux fits suggest method issues. Red-noise tests for QPOs and ZTF/ATLAS validation are planned.

Quantization of a Globally Stable Ghost

Fathe Jalali A., Vikman A., Mukohyama S., and Deffayet C.

Abstract. We canonically quantize a globally stable and dynamically bounded (i.e. no runaways) Hamiltonian system of a physical oscillator coupled non-trivially to a ghost oscillator. Upon quantization, we use standard Rayleigh–Schrödinger perturbation theory to approximate its ground-state and vacuum energy. We then numerically solve the stationary and dynamical Schrödinger equations. We observe convergence of standard perturbation theory and stability of the ground-state over classically long times.

W-Algebras via g_2 Cosets

Guardati E.* and *Procházka T.

Abstract. Two-dimensional quantum field theories with conformal invariance possess an infinite-dimensional symmetry algebra known as the Virasoro algebra. These symmetries can be further extended by higher-spin conserved currents, giving rise to W-algebras. One of the systematic methods for constructing such algebras is the coset construction. We focus on studying W-algebras arising from cosets involving exceptional Lie algebras, such as g_2.

Critical Quantum Dynamics in the Generalized Rabi Model

Kuchař M.

Abstract. Unitary evolution across ground and excited-state quantum phase transitions (ESQPTs) of the generalized Rabi model is analyzed. By numerically solving the time-dependent Schrödinger equation for finite-time interaction ramps, we confirm that ESQPTs stabilize the vacuum in fast quenches and identify additional narrow avoided-crossing traps between two ESQPT energies. This intrinsic non-adiabaticity of the model suggests feasible protocols for observing these phenomena experimentally.

New Interpretation of the Original Charged BTZ Black Hole Spacetime

Hale T., Hull B. R., Kubizňák D., Mann R. B., and Menšíková J.

Abstract. In their seminal 1992 paper, Bañados, Teitelboim and Zanelli (BTZ) proposed a simple charged generalization of what is now known as the spinning BTZ black hole. However, it soon became clear that this spacetime does not satisfy Maxwell equations and was thus discarded. In this presentation, we will see that this incorrect original BTZ metric can actually be redeemed — it can be interpreted as a solution of recently discovered Deshpande–Lunin theory which enables us to construct charged and spinning black holes in all odd dimensions by slightly modifying the action with special topological term.

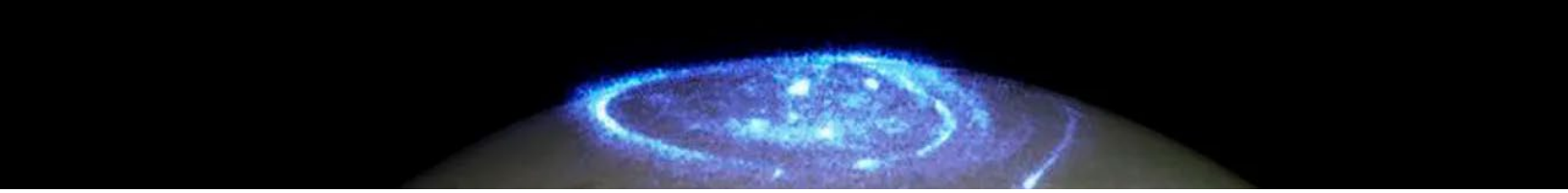

Dynamical Fluctuations in Slowly Manipulated Stochastic Systems

Mlada K.

Abstract. We investigate the dynamical fluctuations of average densities and speed of change in systems undergoing quasistatic transitions. The framework utilised is that of time-dependent Markov processes, with the aim of investigating the functional governing the fluctuations of the densities. The stochastic action for time-averaged occupations is computed, while maintaining distinction between slow (quasistatic) and fast (physical) fluctuation modes. Among the consequences discussed are the Clausius heat theorem and the variational characterisation of slowly evolving states.

Black Holes of Type D and Physical Interpretation of Their Various Forms

Ovcharenko H., Podolský J., and Astorino M.

Abstract. We investigate various metric forms of the Plebanski–Demianski spacetime: the most general solution of the Einstein–Maxwell equations, describing black holes with an aligned electromagnetic field. At first, we present transformations from the new class of Astorino spacetimes (which previously was considered as an independent one) to the previously known forms of the Plebanski–Demianski solution (original form, Griffiths-Podolský, and Podolský–Vrátný ones). Then we investigate the relation of parameters in these forms, and show that various physical parameters (such as acceleration, Kerr, and Taub-NUT rotational parameters) have different interpretations in various metric forms. Moreover, these metric forms allow the resolution of the problem with the existence (or non-existence) of accelerating Taub-NUT spacetime.

Galaxy Evolution in the Virgo Cluster Through Neutral Hydrogen

Partík V., Taylor R., and Minchin R.

Abstract. We study galaxy evolution and the impact of the environment using neutral hydrogen (HI) data from the Widefield Arecibo Virgo Extragalactic Survey (WAVES). HI serves as a tracer of environmental effects and the nearby Virgo Cluster is an ideal laboratory thanks to its proximity and rich population. By comparing galaxies in different parts of the cluster and in the background behind it, we aim to better understand how different environments affect their evolution.

Ultra-high-energy Cosmic Rays from Neutrino-emitting Tidal Disruption Events

Plotko P., Winter, W., Lunardini C., and Yuan C.

Abstract. Revisiting UHECR production in TDEs in light of recent neutrino–TDE associations, we apply an isotropic-emission propagation model to AT2019dsg, AT2019fdr, and AT2019aalc, whose IR dust echoes indicate neutrino generation via cosmic-ray – IR photon scattering. Extrapolated to a full TDE population, we infer a light-to-mid-heavy isotope mix, local rates, and propose enhanced heavy-nuclei acceleration. Predicted diffuse neutrino fluxes are testable by forthcoming radio detectors.

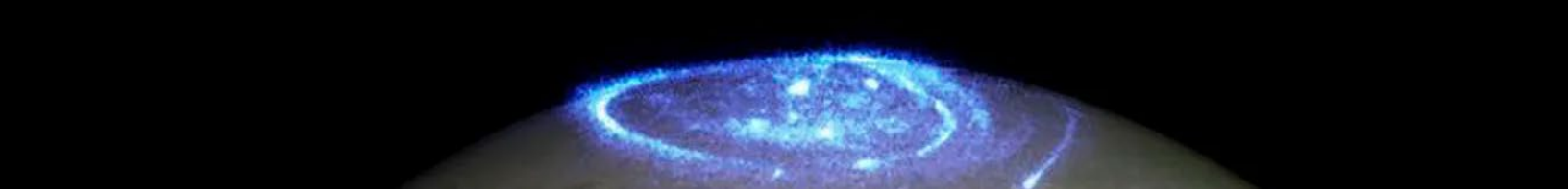

String Field Theory and Boundary Modes

Poletti R.

Abstract. String field theory (SFT) is the field approach to string theory. Its major results include non pertubative computations and proofs of long standing conjectures on the nature of string theory. An important research interest involves a complete undertanding and formulation of an action functional in term of the so called string field, that can be express in BRST formulation. This can be done in a simple way for a theory of purely open strings, while for closed strings the challenges are many, related to the infinite number of interaction terms needed to describe gravity. In this work we start to explain (and solve, at least for the kinetic term) the definition of the SFT action on compact manifolds, which are of fundamental importance in those string theory problems that SFT wants to approach. This requires a definition of some boundary term in the BRST language, to be added to the action preserving the variational principle and the gauge invariance. We prove that this can be done by introducing extra boundary string modes. We finally show that our formalism reproduces the Gibbons–Hawking–York term for gravity in the level one limit of the action.

Hairy Black Holes in Higher-derivative Gravity

Stano M.

Abstract. We investigate static, spherically symmetric solutions in four-dimensional quadratic gravity theories coupled to a conformally invariant scalar field. Motivated by the search for hairy black holes and compact objects beyond general relativity, we consider modifications to the Einstein–Hilbert action via higher-order curvature invariants, such as the Gauss–Bonnet and Weyl terms, with scalar couplings designed to preserve effective conformal symmetries. We analyze key theoretical challenges, including the dimensional constraints and consistency of the field equations. Our aim is to identify viable models admitting exact and physically relevant solutions.

No-hair Theorems for Conformally Coupled Scalar Fields in the Presence of a Cosmological Constant

Voldřich J.

Abstract. We review the status of no-hair theorems for scalar fields in the presence of a cosmological constant. We consider both minimally coupled and conformally coupled scalar fields, which are related through the conformal transformation of the metric. We present some notable solutions and discuss under which assumptions the no-hair theorems apply. We compare some of the solutions with the theorems and show where the latter fail.

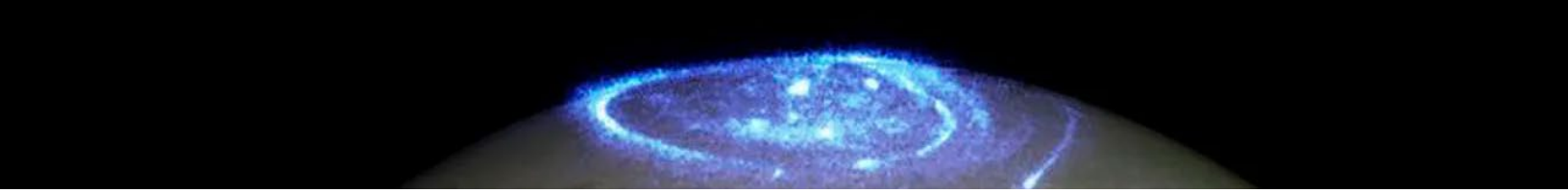

F-2 PHYSICS OF PLASMAS AND IONIZED MEDIA

Multispacecraft Investigation of MHD Turbulence Across Interplanetary Shocks

Abushzada I., Pitňa A., Šafránková J., and Němeček Z.

Abstract. We analyze turbulence across interplanetary shocks using plasma and magnetic field data from ACE, Wind and DSCOVR at L1 point. Using auto- and cross-correlation functions, we examine correlation length, Taylor microscale, and Reynolds number in upstream, downstream, and transition regions. Correlation lengths differ notably, but their ratios are similar. A decrease in Reynolds number across the shock indicates turbulence resetting. Results provide insight into shock-related turbulence evolution.

Calibration of Scintillator-stack Spectrometer at the Microtron MT25 Facility

Agarwal S., Singh S., Devi P., Krupka M., Chvatil D., Garcia A.L., Dudzak R., Krasa J., and Juha L.

Abstract. During high-intensity laser–plasma interactions, bremsstrahlung X-rays are produced, which provide insight into hot electron dynamics. We developed a LYSO crystal-based scintillator-stack spectrometer at the PALS facility, employing FLUKA simulations and an iterative method to unfold plasma temperature. Calibration of such a diagnostic is crucial to validate the measured data. Here, results of calibration measurements are reported, obtained at the microtron MT25 facility in Prague using bremsstrahlung from a 3 mm tungsten converter exposed to 5–8 MeV electrons.

Automated Classification of Near-Earth Plasma Regions Using Plasma and Magnetic Field Data

Aghabozorgi Nafchi M., Němec F., Pi G., Tsai T.-S., and Lee K. H.

Abstract. Machine learning is used to classify near-Earth plasma regions based on 340 days of measurements from the THEMIS-B spacecraft (2008–2010). Input features include plasma velocity, ion density and temperature, magnetic field, and ion energy flux. The random forest model outperforms neural networks in classifying the solar wind, foreshock, magnetosheath, and magnetosphere. Including ion energy flux shows potential for improving the separation between the foreshock and solar wind regions.

High Temperature Vacuum Insulations — Surface Emissivity Measurement

Barton P., Sebik M., and Varju J.

Abstract. The high-performance vacuum thermal insulations are greatly affected by the surface emissivity of the underlying body. Unfortunately, not only are emissivities hard to predict from the common parameters (roughness, material), but they can also vary in time because of transient effects. Therefore, we have measured emissivities of copper, stainless, or nickel-superalloy surfaces with differently processed surfaces, to ensure optimal manufacturing process and best thermal performance of COMPASS-U components.

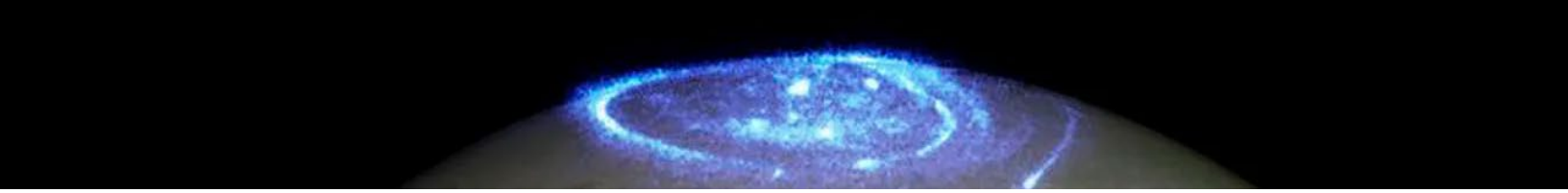

An Overview of Plasma Depletion Events in the Ionosphere of Mars

Basuvaraj P., Němec F., Fowler C., Regoli L., Němeček Z., Šafránková J., Witasse O., and Wilson C.

Abstract. Mars is an unmagnetized planet with a relatively thin atmosphere compared to Earth. However, it has strong remanent crustal magnetic fields, predominantly concentrated in the southern hemisphere. Mars has an ionosphere, made up of ions and electrons, whose structure and composition are influenced by both external (such as solar wind, solar irradiance, and transient space weather events) and internal factors, including planetary rotation and crustal magnetic anomalies. One of the notable ionospheric phenomena recently observed on Mars is the Plasma Depletion Event (PDE)—a large-scale, localized region of reduced plasma density. These structures were first identified by NASA's MAVEN spacecraft. On the dayside, PDEs typically occur above 250 km altitude and are often associated with electrostatic fluctuations, suprathermal electron escape, and energetic ion deposition. In contrast, nightside PDEs, which generally occur below 250 km, remain less understood and are an area of active research. This study explores the occurrence, characteristic features, and potential formation mechanisms of PDEs in the Martian ionosphere, with a particular emphasis on their spatio-temporal extents.

Laboratory Simulations of Hypervelocity Debris Impacts on Fusion Reactor First Walls

Bulička J., Krupka M., Jelínek Š., Burian T., Vaverka J., Dostál J., Dudžák R., Hájková V., Dias T., Carine A., and Juha L.

Abstract. Hypervelocity impacts from micron-sized debris pose a significant threat to first walls and final optics in Inertial Confinement Fusion reactors, and interstellar dust facing instruments on board of space probes, e.g., Comet Interceptor. This talk reviews laboratory scale simulation methods, using light gas gun launchers and laser driven experiments, to mimic such impacts under controlled conditions. It also outlines several novel concepts using short-wavelength (UV/XUV/X-ray) lasers, offering stronger surface absorption; reduced back reflection, scattering, plasma shielding, and hot-electron yield; non-thermal mode of material ablation and tighter energy focus.

High-power-laser Interactions with Foam and Foil Targets: Comparative Studies Using the Filter Stack Spectrometer

Devi P., Singh S., Agarwal S., Krupka M., Garcia A. L., Dudzak R., Švandrlík L., Krása J., and Juha L.

Abstract. An optimized filter stack spectrometer (FSS) is developed to measure bremsstrahlung radiation from foam and foil targets irradiated by sub-nanosecond kilojoule-class laser at the Prague Asterix Laser System (PALS) facility. The FSS instrument has been loaded with aluminium, copper, and lead filters having different thickness alternate with imaging plates in aluminium box shielded by lead. Bremsstrahlung spectra are reconstructed by means of Monte Carlo and Bayesian unfolding, revealing energy distribution and hard x-ray temperatures from Cu foil and foam targets.

Influence of Geomagnetically Induced Currents on Power Line Harmonic Radiation Observed at the Kannuslehto Ground-based Station

Drastichová K., Němec F., Manninen J., and Raita T.

Abstract. We analyze power line harmonic radiation (PLHR) from electrical grids using wave data measured at the Kannuslehto station in Finland. The PLHR spectrum is examined as a function of geomagnetic activity, characterized by local magnetic field variations. Our results show that during quiet periods, PLHR is strongest at odd harmonics. In contrast, even harmonics become more prominent during periods of significant magnetic field variation, associated with stronger geomagnetically induced currents.

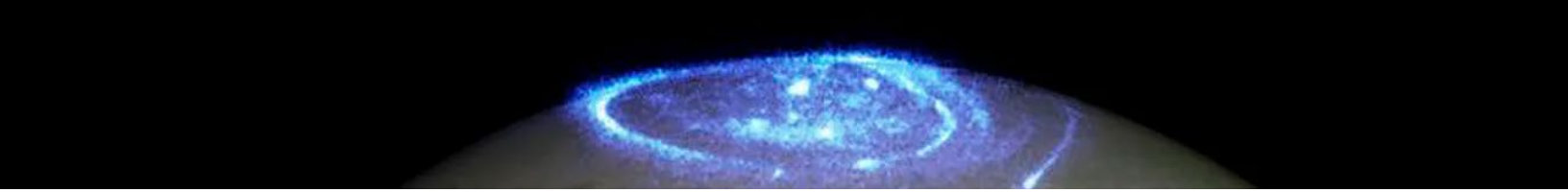

Effect of Cold Atmospheric Plasma on Common Bean Seeds

Khalaf M. *and Medvecká V.*

Abstract. In our work, we studied the effects of plasma produced by diffuse coplanar surface barrier discharge (DCSBD) on Phaseolus beans. The measurements of WCA on the bean seed surface showed a significant decrease in contact angle and improved hydrophilicity for all samples treated by plasma compared to the control sample. The germination parameters of plasma-treated bean seeds were observed for 5 days. Statistical analysis shows that DCSBD treatment is more efficient even after a short treatment time. This work was supported by the Slovak Research and Development Agency within the project under the contract No. APVV-21-0147 and by Slovak Grant Agency VEGA No. 1/0688/22, and Comenius University Grant No.UK/1152/2025.

Surface Modification of Polymers Using Various Low-temperature Plasma Systems

Gahramanli S., Šrámková P., and Zahoranová A.

Abstract. This study investigates the effects of different low-temperature plasma (LTP) systems, Diffuse Coplanar Surface Barrier Discharge (DCSBD), and Piezobrush® PZ3, on the surface properties of polymer substrates. Polyamide, polypropylene, and polycarbonate were treated under controlled plasma conditions, and the changes in surface wettability, chemistry, and morphology were characterized using WCA, ATR-FTIR, XPS, and SEM. This research shows the effectiveness of LTP systems in polymer surface engineering and provides a selection of applications. Keywords Low-temperature plasma, polymers, Surface modification, DCSBD, piezoelectric discharge, WCA

Electron Induced Dissociative Excitation of Formamide

García E., Stachová B., Matejčík Š., and Országh J.

Abstract. Formamide, the simplest amide, is an interesting system to study due to its diverse chemistry includes functional groups and chemical bonds found in key biomolecules, making it a candidate as a potential precursor to life. The emission spectrum following electron impact on formamide is studied in a crossed-beam experiment. The spectra were measured at three slit widths of 100 and 300 μm, all at 50eV, within a wavelengths range of 280 to 1000 nm, to achieve optimal ratio of signal intensity and resolution. In the emission spectra, several lines and bands could be successfully identified, where the most prominent excited species that found were the hydrogen Balmer series, the nitrogen triplet system NH, the excited CH radical in the A and B electronic states, and atomic oxygen.e excited CH radical in the A and B electronic states, and atomic oxygen.

A Comprehensive Study of Plasma Parameter Changes in the Magnetopause Boundary Layer

Ghosh M., Pi G., Šafránková J., and Němeček Z.

Abstract. Magnetopause plays a vital role in the magnetospheric system, regulating the flow of mass, energy, and momentum from the solar wind into the Earth. The THEMIS mission, launched in 2007 to study the substorms, has been observing the magnetopause for nearly two decades. This study aims to provide a comprehensive understanding of the structure and profiles of plasma parameters in the magnetopause boundary layers. Various plasma parameters exhibit structural variations inside the boundary layers.
A superposed epoch analysis shows a distinct peak in the Y-component of the ion velocity in the magnetopause boundary layer that can be associated with the Chapman–Ferraro current system.

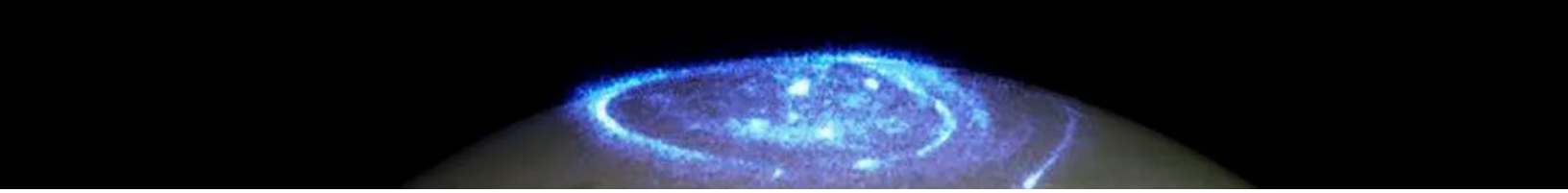

Experimental Design for Studying Ammonia Deuteration Mechanisms in Interstellar Conditions

Hernandez Alvarez O. E., Rednyk S., Roučka Š., Dohnal P., Plašil R., and Glosík J.

Abstract. Our ongoing research explores the deuteration pathways of ammonia under low-temperature interstellar conditions. We present the experimental design for investigating reactions between NH_3 and D_3^+ using a 22-pole cryogenic ion trap, with future plans to extend measurements to even lower temperatures via a supersonic beam setup. Preliminary measurements demonstrate reaction rate coefficients at temperatures around 200 K, while our apparatus is being optimized to reach temperatures below 180 K. This work-in-progress aims to validate theoretical models and develop new experimental capabilities for studying fundamental astrochemical processes.

Particle Simulation of Solar Wind Electron Plasma Wave Growth

Houfek P., Souček J., and Santolík O.

Abstract. We present results of particle-in-cell simulations of the growth of electron plasma waves due to beam-plasma instability. We give a brief introduction to waves and electron instabilities observed in solar wind followed by an introduction to the simulation model. In the simulation we investigated the growth of waves for different beam properties (cold dense beam and hot tenuous beam). We have successfully reproduced both the initial linear growth and later saturation of the instability.

EIT with Ion and Electron Confined in a Paul Trap

Hudák I., Kumar V., Lausti N., and Hejduk M.

Abstract. Electromagnetically induced transparency (EIT) provides a versatile link between optical and radio-frequency transitions in trapped ion–electron systems. In this study, we investigate its implementation for Ca^{2+} confined in a Paul trap. We calculate the absorption profile of the chosen probe transition and analyse how an integrated fiber–facet microcavity, operated at that optical frequency, responds when a radio-frequency field is applied. The RF field alters the cavity's transmission spectrum, which can then be measured through a controlled frequency scan.

Power Spectral Analysis of Dust Distribution in Saturn's Rings from Cassini RPWS Observations

Ijaz S., Nouzak L., Pavlu J., Němec F., Pisa D., Vaverka J., Němeček Z., and Šafránková J.

Abstract. We present a study of dust distribution in Saturn's rings, analyzing dust impact signals detected by the Radio and Plasma Wave Science (RPWS) instrument aboard the Cassini spacecraft. Over its 13-year mission, Cassini's RPWS antennas detected numerous short, spiky signals associated with hypervelocity dust impacts during multiple ring-plane crossings. Our work focuses on the analysis of these signals between radial distances of 2.45 to 4.5 Saturn radii (R_S), covering key regions such as the G and E rings. The derived profiles from the power spectral method are consistent with those obtained via a waveform-based event identification routine, supporting the robustness of the spectral approach. The study indicates that the profiles can be modeled by a Gaussian distribution, with thicknesses ranging from 900 km in the dense, narrow G ring to 5000–9000 km in the wide E ring. These results offer new insights into the spatial structure of Saturn's dusty rings and highlight the utility of power spectral analysis as an alternative approach for analyzing dust impacts in planetary environments.

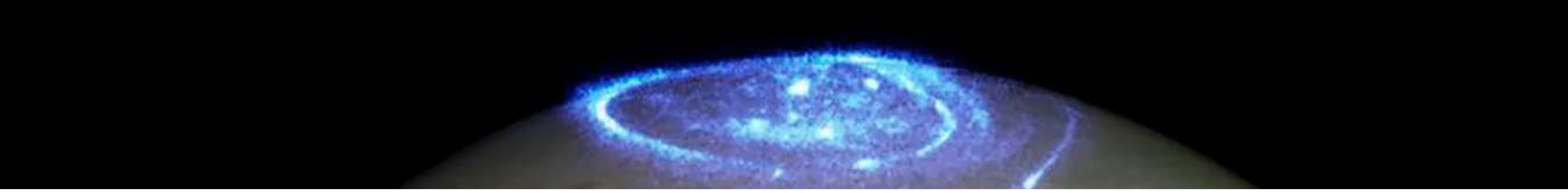

Instrumented High Fluence Neutron Irradiation Test of Antimony Hall Sensors — Experimental Setup and the First Results

Ivanek M., Duran I., Entler S., Sladek P., Soltes J., Viererbl L., Melichar T., Reboun J., Turjanica P., Simonovsky M., Stepan L., and Bankov R.

Abstract. Hall sensors based on antimony sensitive layer will be installed on ITER within the system of Outer Vessel Steady-state magnetic field Sensors (OVSS) and they are also considered for deployment on future European demonstration fusion power reactor (EU-DEMO). The role of these sensors will be to contribute to determination of the key tokamak plasma parameters such as the plasma position, shape, and plasma current. Ensuring sufficient stability and robustness of the sensors under radiation loads, expected to be particularly high on EU-DEMO, is one of the key design drivers and challenges. This contribution presents the design of an instrumented high fluence neutron irradiation experiment, where antimony Hall sensors will be exposed to neutron and gamma radiation in the LVR-15 research reactor. Sensitivity, input/output resistance and temperature of each Hall sensor will be monitored continuously over the course of irradiation. The contribution discusses design choices and technological solutions for this irradiation experiment.

Characterization of Non-Gaussian Beam Profiles Using Laser Ablation

Jelinek S., Dudzak R., Burian T., Dostal J., Hajkova V., Juha L., Krupka M., Makita M., Tavakkoly M., Vannoni M., Vozda V., Wild J., and Chalupsky J.

Abstract. We characterized fluence distributions [J/cm^2] of focused non-Gaussian laser beams using the ablation imprints method. It is derived from the Liu's method which is limited to measuring beam widths of Gaussian laser beams. Another advantage of the ablation imprints method is its high dynamic range ($\approx 10^{-3}$). We combined it with far-field imaging to accurately evaluate the fraction of the pulse energy contained in low-fluence beam tails which increases the accuracy of the peak fluence determination.

Rovibrational Overtone and Combination Bands of the $HCNH^+$ Ion

Kassayová M., Jiménez-Redondo M., Sarka J., Dohnal P., Glosík J., Caselli P., and Jusko P.

Abstract. The $HCNH^+$ ion, relevant in interstellar chemistry, was studied in the 6200–6900 cm^{-1} range, focusing on overtone and combination bands of N–H and C–H stretches. Even very weak bands, such as $v_2 + v_3 + 2v_5^0$, were detected using a "kick-out" LIR scheme. The endothermic reaction with C_2H_4 led to products that further reacted to form $C_5H_7^+$, which was used as the spectroscopic signal.

Observing Lightning Initiation from Orbit: A Multisystem Case Study

Kolinska A., Kolmasova I., and Santolik O.

Abstract. We investigate lightning initiation by combining optical data from the Lightning Imaging Sensor (LIS) aboard the International Space Station with ground-based broadband electromagnetic measurements. Our case study analyzes 11 lightning flashes (2020–2023) using data from SLAVIA magnetic detectors across Europe, along with ENTLN, WWLLN, EUCLID, and the SAETTA Lightning Mapping Array. Results show that optical emissions from the preliminary breakdown phase are clearly detectable from low Earth orbit, showing the value of space-based observations in studying lightning initiation.

Melnikov Integral Method for Description of Magnetic Footprints

Kripner L. and Cahyna P.

Abstract. In a tokamak, non-axisymmetric perturbations replace the separatrix with stable and unstable manifolds, forming magnetic footprints on plasma-facing components. Field line tracing and Hamiltonian mapping describe these structures. We present a simplified method using the Melnikov integral to describe magnetic footprint boundaries, making it ideal for studying systems with many degrees of freedom, such as those with RMP coils.

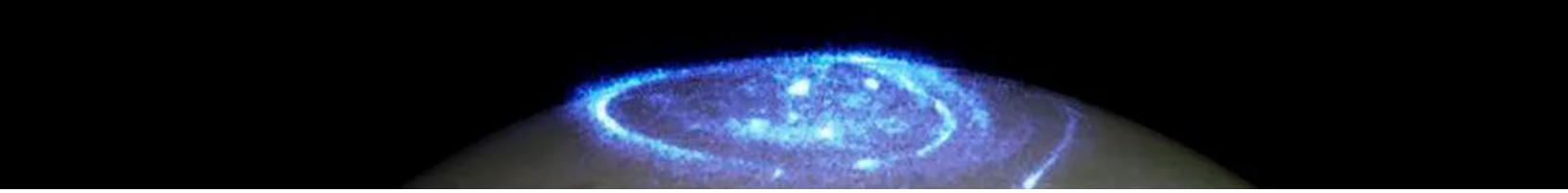

Roadmap of $e^- + {}^{40}Ca^+$ Dual Trapping @ UPLP

Kumar V., Lausti N., Hudák I., Motyčka D., Jelínek A., Přiklenk O., Rádek R., Mahmoudi P., Tarana M., and Hejduk M.

Abstract. We are constructing a system to simultaneously trap $e^- + {}^{40}Ca^+$ in a dual-frequency Paul trap operating at room temperature. The goal is to enable microwave signal detection, using electron–ion coupling as a sensing mechanism. The system employs a 3D-printed coaxial trap with GHz confinement for e^- via a λ/2 resonator, and MHz end-cap drive for ${}^{40}Ca^+$ trapping. We use a 3D-printed atomic source to generate ${}^{40}Ca$ atomic beam, and a two-color scheme for $e^- + {}^{40}Ca^+$ loading in the Paul trap. Currently, we are in the process of calibrating and tuning our laser systems for the Doppler cooling of ${}^{40}Ca^+$ ions, targeting the $4s^2\ S_{1/2} \rightarrow 4p^2\ P_{1/2}$ transition using UV laser at 396.847 nm. To prevent optical pumping into the metastable D-state, we employ an IR repump laser at 866.214 nm to drive the $3d^2\ D_{3/2} \rightarrow 4p^2\ P_{1/2}$ transition. Additionally, for neutral ${}^{40}Ca$ atoms photo-excitation, we use ${}^{40}Ca(4s^2\ {}^1S_0) \rightarrow {}^{40}Ca^*(4s4p\ {}^1P_1^o)$ at 422.792 nm as the step towards loading. Alongside these efforts, we are progressing on our integration roadmap, which includes the design and fabrication of 2D chip-based Paul traps.

ACKNOWLEDGMENTS. This work is supported by the Czech Science Foundation (GAČR: GA24-10992S), the Charles University Grant Agency (GAUK 295023, and GAUK 131224), the Czech Ministry of Education, Youth, and Sports (project QM4ST, reg. no. CZ.02.01.01/00/22_008/0004572), and the Technology Agency of Czech Republic (TAČR: TN02000020). We also acknowledge previous support from the Primus Research Programme (PRIMUS/21/SCI/005).

Dynamics of Small 2D Coulomb Crystals

Lausti N., Kumar V., and Hejduk M.

Abstract. Laser-cooled trapped ions in Coulomb crystals are used in quantum technology. Precise information about their vibrational modes is needed in determination of laser frequencies in a trapped-ion quantum computer. Multidimensional crystals display some advantages for this application, but dynamics of such quantum many-body systems has been studied very little. We present a systematic study of vibrational modes for crystals with up to 7 ions in the potential of our coaxial Paul trap.
The geometries are solved by a FEM software, and the vibrational modes are found by FFT. We also evaluate the melting points of such crystals. As all point Paul traps have roughly similar shape of potential, the results can be used as a guideline for different devices.

Geostationary Satellite Observations of Magnetosphere During 2024 Mother's Day Weekend Magnetic Storm

Li S., Pi G., Němeček Z., and Šafránková J.

Abstract. The geomagnetic storm over Mother's Day weekend (10–11 May 2024) ranks among the strongest in recent decades. This study presents three major findings. First, we identified 62 dayside magnetopause crossings and evaluated four magnetopause models (Lin et al. 2010; Shue et al. 1998; Petrinec and Russell 1996; Li et al. 2023). Their root-mean-squared deviations are 1.57, 1.61, 2.27, and 1.30 RE, respectively. Second, the Energetic Heavy Ion Sensors on GOES-16 and GOES-18 detected increased helium fluxes around 15:00 UT. Two helium peaks were observed during the storm, possibly indicating ICME structure. Third, as the ICME impacted the magnetosphere, FengYun-4B was in the magnetotail and recorded repeated north–south magnetic field changes. About 12 hours later, GOES-16 and GOES-18 observed three southward magnetic field segments in the tail.
Dipolarization fronts may have been compressed below geostationary orbit (6.6 RE). MHD simulations from the Space Weather Modeling Framework complement these observations. Our results show that geostationary satellites can probe magnetospheric structure under extreme solar wind conditions.

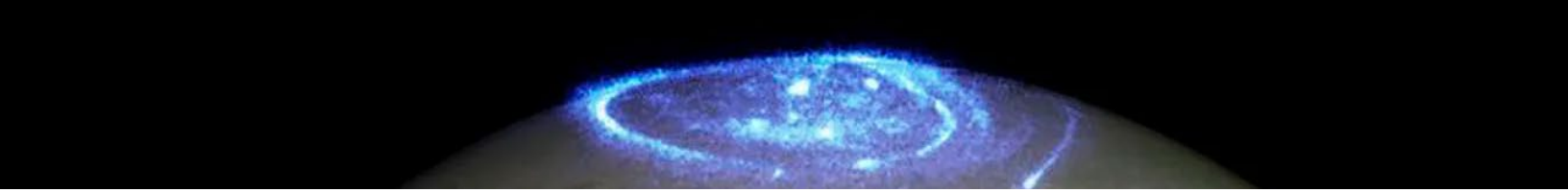

Automatic 3D Reconstruction of Coronal Mass Ejection Based on Dual Viewpoint Observations and Machine Learning

Lin R., Yang Y., Shen F., Pi G., and Li Y.

Abstract. We have developed an algorithm that automatically reconstruct CME structure integrating dual-viewpoint observations with machine learning techniques. It consists of three stages: (1) region acquisition, (2) model construction, and (3) function optimization. First, we use two independent Convolutional Neural Networks (CNNs) to identify and detect CMEs in the coronagraph images from two spacecrafts. Next, we construct the projections of Graduated Cylindrical Shell (GCS) model in the fields of view (FOVs) of the coronagraphs. In the final step, optimal parameters are retrieved optimizing the function that quantifies the morphological discrepancies between the image of GCS model and the CME detection. A statistical analysis on 128 CME events is conducted to investigate both the two-dimensional (2D) and three-dimensional (3D) parameters. The proposed method can further be used to provide CME initial parameters for magnetohydrodynamics simulations, enabling a deeper understanding of CME kinematics.

Detection of Lightning-generated Whistlers in DEMETER Satellite Data

Linzmayer V., Němec F., Santolík O., and Kolmašová I.

Abstract. We focus on the automated detection of lightning-generated whistlers in satellite data. We use burst mode data measured by the electric field instrument ICE onboard the DEMETER micro-satellite. Using a manually labeled training dataset of whistlers, we train a YOLOv11-m object detection model to detect whistlers in power spectral density spectrograms. We demonstrate the effectiveness of the identification routine and present preliminary statistics on whistler occurrence.

Low Energy Electrons Interaction with Acetone (CH3)2CO in the UV-Vis Spectral Region

Megersa G. D.*, Stachová B., Garcia Angulo E. L., Matejčík Š., Michalczuk B., and Országh J.

Abstract. This study investigates the interaction of acetone molecules with low-energy electrons (10–100 eV) using emission spectroscopy in the UV-Vis spectral region, with a focus on spectral analysis and the determination of emission cross-sections. The primary objective is to obtain data on the electron-induced fluorescence of (CH3)2CO molecules, which are significant components of many extraterrestrial objects and hold substantial potential in astrophysical research. The processes of electron impact fluorescence methods enable the study of the electronic, vibrational, and rotational state of molecules, as well as the exploration of dissociation excitation, ionization, and photon emission processes.

Impact of Spherical Cathode Geometry on Plasma Behaviour and Space-charge Structures

Mekki R. N., Enescu F., Ionita-Schrittwieser C., Schrittwieser R., Hubička Z., and Tichý M.

Abstract. This study examines plasma behavior in a concentric spherical hollow cathode discharge using optical emission spectroscopy. It focuses on the formation of complex plasma structures, such as sphere- and fireball-like regions, emerging from a single-orifice spherical cathode. Spatial profiles of electron temperature and density reveal the dynamics of space-charge formation and plasma propagation, demonstrating potential for efficient ion acceleration in advanced plasma technologies.

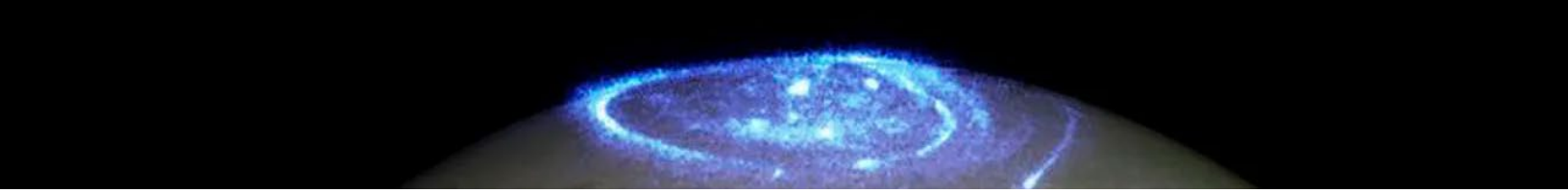

Statistical Analysis of Waves in Solar Orbiter RPW-TDS Data

Mičko J., Souček J., Píša D., and Santolík O.

Abstract. RPW-TDS instrument onboard Solar Orbiter spacecraft provides measurements of plasma wave and dust events. We attempt to combine two datasets — waveform snapshots (TSWF) and on-board statistics (STAT) provided by the instrument to produce a new STAT-TS dataset. TSWF dataset contain full waveform snapshots of selected events detected by an onboard algorithm while STAT dataset contains basic information about all events recorded by the instrument. In our work, we attempt to classify waves identified by onboard algorithm as either Langmuir or ion acoustic waves. However, the observations might be influenced by spacecraft interference resembling natural waves. We developed a technique to filter out data affected by the interference and thus greatly improved the statistics. Based on the current STAT-TS dataset version, we present our results for years 2022 and 2023.

Plasma Diagnostics in He–N_2–CO_2 Magnetron Discharge: A Synergistic Approach Using OES and Quantum Circuits

Mishra H., Tichy M., and Kudrna P.

Abstract. This study presents the measurement of fundamental plasma parameters — namely excitation temperature, electron density, and rotational and vibrational temperatures — in a non-segmented cylindrical cathode magnetron using optical emission spectroscopy (OES). A gas mixture composed of helium, nitrogen, and carbon dioxide in a 3:2:1 ratio was employed to investigate plasma behaviour under the influence of an external magnetic field. The primary objectives are twofold: (1) to evaluate the effects of the He+N_2+CO_2 admixture on plasma characteristics, and (2) to explore the integration of a quantum circuit protocol from the perspective of classical plasma diagnostics. Plasma parameters were analysed as functions of varying magnetic field strength (Tesla), discharge current (mA), and pressure (Pa), while maintaining a constant gas flow rate (sccm). The results contribute to a deeper understanding of complex gas-phase plasma interactions and the potential crossover between quantum computation and conventional plasma analysis.

Characterisation of the HiPIMS Process for $CuFe_2O_4$ Spinel Deposition

Naiko I., Ostapenko A., Čada M., Venkrbcová I., and Hubička Z.

Abstract. Ferrites with a spinel structure have been reported to boost cost-effective hydrogen evolution in water splitting, a method of conserving renewable energy. In our research, copper ferrites were prepared using reactive HiPIMS discharge with different pulse lengths. The ion fluxes of all the investigated modes showed that their magnitudes were independent of pulse length but shifted to later times as the pulse length increased. At the same time, pulse energy was found to have a crucial impact on the deposited thin films properties.

Langmuir Probe Sheath Dynamics Under Medium Pressure

Palacký J. and Roučka Š.

Abstract. This study investigates the sheath size time evolution of a cylindrical Langmuir probe using a 2D3V particle model of low-temperature plasma under an external electric field. The probe potential was set positive relative to the plasma potential, and the stabilization of the sheath around Langmuir probe after a sudden change of the probe potential was observed.

Tebuconazole Degradation Using Diffuse Coplanar Surface Barrier Discharge

Pardo A., Klas M., and Matejcik S

Abstract. Due to their high persistence, triazole fungicides such as tebuconazole can remain in food even after harvest, posing a potential risk to human health. Therefore, the development of effective technologies to remove these residues is essential to improve food safety. The diffuse coplanar surface barrier discharge was selected for its scalability in real-world applications, achieving 60% degradation in just 10 seconds of treatment using 450 W. The degradation was quantified using an ion mobility spectrometer

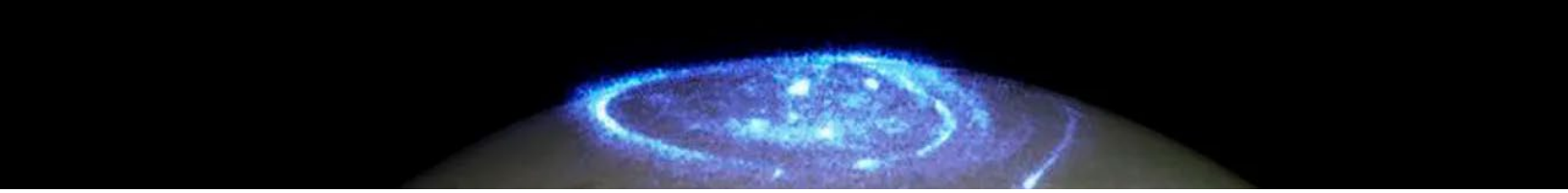

Response of Electron Distribution to Interplanetary Shock with Solar Orbiter Observations

Park B., Pitňa A., Šafránková J., and Němeček Z.

Abstract. Electrons are ubiquitous in solar wind plasma playing a significant role in small-scale turublence as well as ions. Consisting of thermal core, superthermal halo, and cold beam (often addressed as 'strahl'), the electron distributions are recently investigated in terms of their evolution in the inner heliosphere and through interplanetary shock using high-accuracy instruments such as SWA-EAS aboard the Solar Orbiter spacecraft. While the precise orgin of each electron population is poorly understood, the response of the electron distributions to interplanetary shock is expected to reveal the mechanisms of energy transfer amongst the populations in small scales. We present a statistical analysis of Solar Orbiter SWA-EAS electron velocity distributions across interplanetary shocks, and compare the evolution of the electron parameters with those observed in the pristine solar wind. We priliminarly suggest that super-thermal halo population decreases with increasing kappa values across shock and leads to the heating of the core population. We will extend the current study toward the Earth's bow shock where high-Mach numbers (representing a strong shock) are typically observed.

Full-Wave Modeling of Whistler Wave Going Through Martian Ionosphere

Rosická K., Santolík O., Němec F., and Kolmašová I.

Abstract. Lightning flashes have been observed on several planets in the Solar System. However, atmospheric discharges have not yet been detected on Mars, despite theoretical models predicting their occurrence within dust devils. We present a full-wave simulation of an electromagnetic signal generated by a hypothetical lightning discharge. We show that it can exceptionally propagate through the Martian ionosphere in the form of a whistler, which would be detectable by a spacecraft orbiting Mars.

Dissociative Electron Attachment to Iodomethane

Saha S., Fedor J., and Nag P.

Abstract. Low-energy electron molecule scattering often leads to the formation of anionic states via resonant electron capture, which may result in dissociative electron attachment (DEA).
In J. Heyrovsky institute, we have a unique DEA-VMI (velocity map imaging) spectrometer combined with a trochoidal electron monochromator [1]. Recently, we studied DEA to iodomethane (CH3I) using the DEA-VMI spectrometer. We observed three fragments due to DEA, I^-, CH_2^- and CH^-. To know the angular and kinetic energy distributions we measured the velocity map images of I^- fragments around the zero eV resonance and around the second resonance at 8.5 eV. For ions exhibiting resonance near zero eV, a strong angular distribution is observed, with ions predominantly formed in the forward and backward directions. Whereas for 8.5 eV resonance we saw isotopic angular distribution. We also measured the kinetic energy distribution of the I^- fragments for all the four different incident electron energies and it showed a peak around 0.07 eV. References:
1. P. Nag, M Polášek, J. Fedor (2019) Phys. Rev. A, 99, 052705.

Study of the Proton Beam Parameters Near the Sun

Satyasmita Sruti, Ďurovcová T., Němeček Z., and Šafránková J.

Abstract. The solar wind often shows two proton populations: a dense proton core and a faster, less dense proton beam. The proton beam relative abundance is typically 10–20 %, and it drifts relative to the core along the IMF at about 1.2 local Alfven speed. The origin and evolution of the proton beam is not yet fully understood. A previous study based the Helios data suggests that the seed of the proton beam forms close to the Sun. We investigate the radial evolution of various proton beam parameters observed by the Solar Probe Cup from 0.1 to 1.0 AU and discuss possible reasons for their behavior.

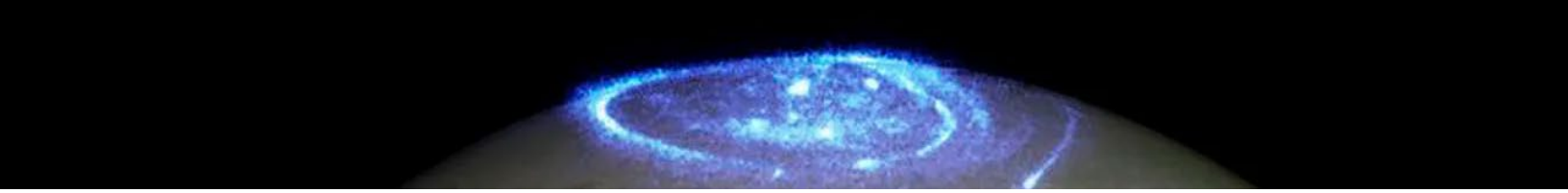

Dissociative Recombination of HCO^+ Ions with Electrons in the Temperature Range of 80–200 K

Slezak P., Kassayova M., Dimitru S., Rednyk S., Plašil R., Roučka Š., Dohnal P., and Glosik J.

Abstract. Dissociative recombination of the HCO^+ ion in the temperature range 80–200 K was investigated using a Stationary Afterglow with Cavity Ring-Down Spectroscopy (SA-CRDS) apparatus complemented by microwave plasma diagnostics. This configuration enabled high sensitivity and temporal resolution in the simultaneous detection of recombining ions and electrons. The measured rate coefficients display a pronounced temperature dependence, which is critical for accurate modeling of chemical processes in cold interstellar environments. A chemical kinetics model was developed to quantitatively interpret the experimental data.

Electron Density Measurements in Low-pressure Hollow Cathode Plasma Jet System

Tuharin K., Mishra H., Turek Z., Tichý M., and Kudrna P.

Abstract. Electron density is a critical parameter in characterizing processing plasmas, significantly affecting properties such as deposition rate and uniformity. In this study, we investigate electron density in a low-temperature plasma using a cutoff probe and compare the results with those obtained from hairpin and Langmuir probes. All measurements were carried out in a DC discharge produced by an iron hollow cathode [1], under consistent experimental conditions. This comparative approach offers valuable insights into the accuracy and consistency of electron density measurements across different diagnostic techniques. The measurements were performed in an argon–oxygen gas mixture at a low pressure of 5 Pa, examining the dependence of electron density on discharge current and the $Ar:O_2$ ratio. Keywords: Cutoff probe, Hairpin probe, Langmuir probe, DC discharge

Investigation of Plasma–Material Interactions on Different Substrates Using a Hot Tungsten Cathode System Under Low-pressure Conditions

Turek Z., Mašek T., Mishra H., Tichý M., and Kudrna P.

Abstract. We present a hot tungsten cathode system to study the interactions between low-temperature plasma and thin metal layers sputtered onto both conductive and non-conductive substrates. This research aims to understand material selection for LMD divertor applications. Before interaction in the hot cathode system, we prepared three series of samples using high power impulse magnetron sputtering.

Measurement of the CMOS Chip Sensitivity

Uvarova L., Novak F., and Mureşan M.

Abstract. The study of CMOS chip sensitivity was done within the investigation of the remote scanning capabilities for in-situ damage detection for further utilization in the LIDT (laser induced damage threshold) measurements. Results for two configurations of setup (with movable lens and standard) and lenses with different focal distances (200, 500, and 750 mm) were compared.

Heating of Optical Elements Exposed to Intense X-rays Inspected by NIR Thermal Camera

Valdová Z., Bulička J., Burian T., Chalupský J., Vagovič P., and Juha L.

Abstract. NIR thermal camera was used for monitoring of a temperature on surfaces of selected optical elements heated by ultra-short x-ray laser pulses at the European XFEL facility. Earlier, synchrotron-radiation heated beam splitter was inspected using the same camera at ESRF. Understanding thermal behaviour of different elemental solids exposed to intense x-ray radiation can help to find conditions under which x-ray optical systems can be operated at those facilities without any risk of irreversible damage or even just a temporary loss of their full functionality.

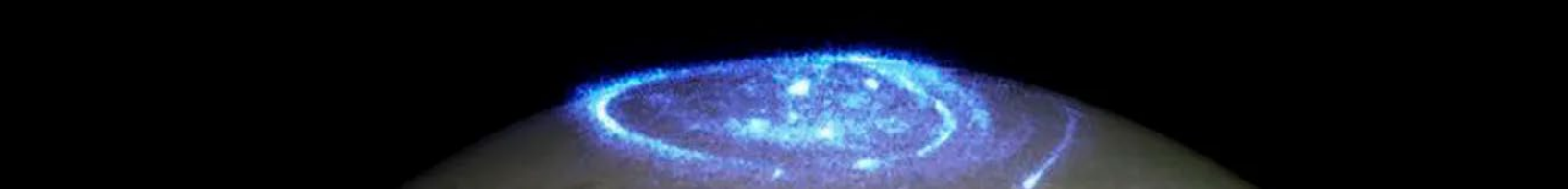

Early-phase Effects of an ELM in JET

Vrba Š. and Tskhakaya D.

Abstract. We use the fully kinetic Particle-in-Cell Monte Carlo code BIT1 to simulate the SOL of the JET tokamak during the onset of ELM activity. We briefly describe our simulation model, then we present the simulation results and analyze the immediate effects of the ELM — within the first 10% of its duration. These include the temporal evolution of plasma and impurity profiles — such as density, temperature, and potential — as well as particle and heat fluxes to the divertors and tungsten sputtering.

Connection of the Magnetosheath Jets with the Foreshock Activities

Xirogiannopoulou N., Goncharov O., Safrankova J., and Nemecek Z.

Abstract. Plasma structures with an enhanced dynamic pressure, known as jets are often observed in the Earth's magnetosheath. These structures are more often detected downstream of the quasiparallel bow shock, i.e., behind the foreshock. This region is dominated by waves and reflected particles which interact with each other and create different transients. Xirogiannopoulou et al. (2024) found that the subsolar foreshock contains several types of structures with enhanced density or/and magnetic field magnitude — plasmoids, SLAMS and mixed structures. Many previous studies established that some of these foreshock structures can be a source of magnetosheath jets (Raptis et al., 2022). Following these results, we use data collected by the cross-calibrated THEMIS spacecraft and present multi-spacecraft case studies of the connection between the foreshock and magnetosheath structures. According to our observations, we suggest that the generation of magnetosheath jets is associated with some additional mechanism from the ones we know (ex. BS ripples) that is more complicated or the knowledge we have is incomplete.

A Novel Method for Estimating Geomagnetically Induced Currents in Power Grids During Geomagnetic Disturbances

Zhang X., Yu N., and Pi G.

Abstract. Geomagnetic storms induce geomagnetically induced currents (GIC), threatening power systems. Traditional GIC calculation methods integrating geoelectric fields accumulate errors. We propose a novel approach: modeling transmission lines in 2D and inverting line voltages using geoelectric fields to enhance accuracy. A genetic algorithm optimizes measurement points, reducing system ill-posedness. We also integrate real-time local conditions (temperature, wind speed, icing) into GIC estimation and analyze sensitivity. The study explores GIC-substation site selection links in Guangxi, recommends DC monitoring devices, and examines extreme climate impacts on GIC. Validation uses Guangdong–Guangxi grid examples.

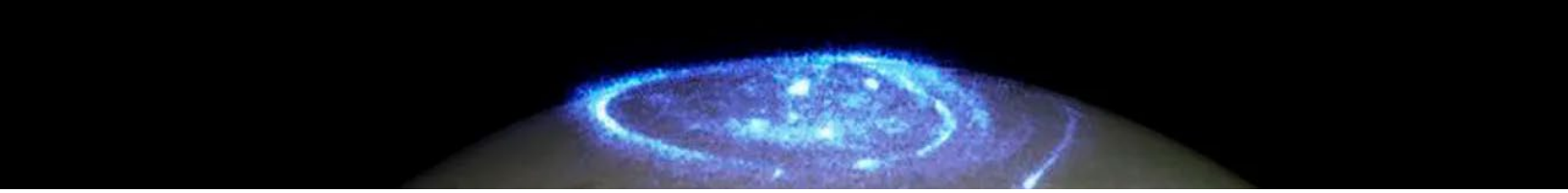

F-3 PHYSICS OF CONDENSED MATTER AND MATERIAL RESEARCH

Scalable Effective Models for Complex Superconducting Nanodevices

Bobok D., Frk L., and Žonda M.

Abstract. We have derived a Chain Expansion (ChE) method that maps superconducting leads onto finite chains for systems well described by the Superconducting Anderson Impurity Model (SCIAM). We show that ChE-based effective models closely match the Numerical Renormalization Group (NRG) solutions of the full SCIAM across a broad parameter range, already for short chains solvable via Exact Diagonalization (ED). The one-dimensional nature of ChE enables the use of effective models with longer chains, inaccessible to ED, via the Density Matrix Renormalization Group.

Superfluid Weak Links and the Precise Detection of Rotation and Flows

Gheorghe A., Danylchenko P., Harašta S., and Schmoranzer D.

Abstract. In superfluid quantum interferometry, operating much like the current oscillations in a DC SQUID, oscillatory flows at the weak-link interface between two helium containers under a chemical potential open the door to studying Sagnac interferometry, phase slip behavior, and gradient meters as potential measuring tools. These may serve as a launching platform for a wide range of superfluid experiments. Ongoing work in our department focuses on advancing sensing and fabrication techniques.

Growth and Characterization of Flat Layered MoS_2 and Co_9S_8 Thin Films by Modulated Elemental Reactants Molecular Beam Epitaxy

Peheliwa V. M., Vinnik O., Kratochvílová M. H., and Verhagen T.

Abstract. We report the synthesis of ultrathin MoS_2 and Co_9S_8 thin films using modulated elemental reactants molecular beam epitaxy (MER-MBE). The principle of the MER-MBE growth is explained for the Co-S system. Via precisely tuning the sulfur concentration, flat Co_9S_8 layered architectures with enhanced in-plane ordering can be grown, as validated by optical, scanning electron and atomic force microscopy and X-ray diffraction. Similar, MoS_2 thin films (with thickness varying between 5–50 layers) were grown. MoS_2 adopts the 2H polytype,however the surface becomes more rough as the number of layers increases These results confirm that sulfur and layer thickness control in Co_9S_8 and in MoS_2 are critical for growth of ultra-flat 2D materials engineering, with applications in catalytic and quantum technologies among others.

Martensitic Transformation in Titanium and Zirconium Alloys

Salata K., Bastl E., Capek J., Knapek M., Strasky J., and Harcuba P.

Abstract. This work investigates deformation mechanisms in metastable β-titanium and zirconium alloys with enhanced ductility, focusing on martensitic transformation and twinning. The main experimental techniques used to study these mechanisms are tensile testing, XRD, and EBSD. Preliminary results from binary Ti-12Mo, Ti-15Mo alloys will be presented.

Stochastic Transitions in Quasi-two-dimensional Quantum Turbulence

Talíř M., Novotný F., and Varga E.

Abstract. In this work, we study quasi-two-dimensional turbulence in He II, a two-fluid liquid consisting of viscous normal fluid and an inviscid superfluid where circulation is quantized. We confined He II to nanofluidic cavity supporting superfluid Helmholtz resonance, and observed the transition to fully developed quasi-2D quantum turbulence, which we found that occurs through memoryless stochastic transitions between multiple turbulent states.

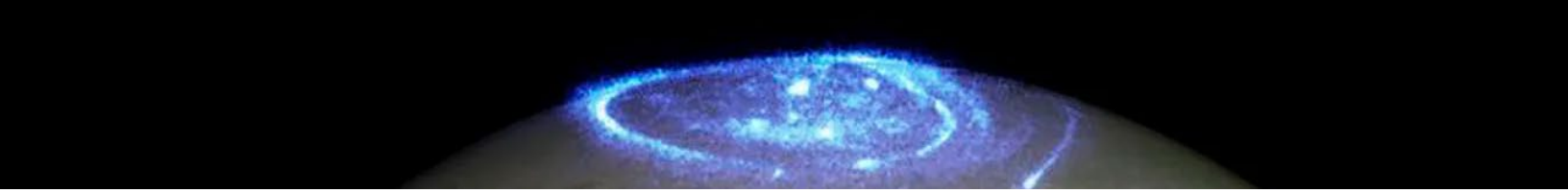

Gamma Point Magnons in Antiferromagnetic Alpha-MnTe

Tázlarů S., Erlingsson S. I., Orlita M., and Výborný K.

Abstract. Semiconducting and altermagnetic manganese telluride (MnTe) is a promising material for spintronic applications. Bulk alpha-MnTe low temperature gamma point (k=0) magnon mode was measured using THz spectroscopy techniques for various canting angles of the applied magnetic field vector from the sample hard-axis, and its observed behaviour was investigated. Linear spin wave theory (LSWT) model was utilized to interpret the measured data and determine out-of-plane magnetic anizotropy.

Preliminary Study on Hydrogen Embrittlement in As-extruded Titanium Alloys Ti-6Al-4V and Ti-0.3Mo-0.8Ni

Wiśniewski M., Drozdenko D., and Dobroň P.

Abstract. Exposure to hydrogen environments leads to the degradation of mechanical properties in metals, often resulting in brittle fracture under load. This phenomenon is known as hydrogen embrittlement. Pilot studies were performed on two commercially used titanium alloys: Ti-6Al-4V and Ti-0.3Mo-0.8Ni, both in the as-extruded form and in pre hydrogenation stage. The scope of the study included microstructural and crystallographic texture analysis using electron microscopy techniques (SE, BSE, EBSD), as well as compression testing combined with acoustic emission technique.

F-4 BIOPHYSICS, CHEMICAL AND MACROMOLECULAR PHYSICS

Utilizing Flexible Polymer Linkers in a Continuous Monitoring Plasmonic Biosensor for Detecting Low Molecular Weight Analytes

Aktug G., Asai N., Van-Truc, V., P. Asokan, Huang C-J, Monteiro da Santa, C., Park, S., Sergelen, K., and Dostalek J.

Abstract. Plasmonic sensor for continuous low molecular weight analyte (e.g., therapeutic drugs) monitoring. Reversible analyte-ligand interaction with plasmonically enhanced fluorescence (PEF) energy transfer readout. Flexible polymer linker (FPL) connects surface-immobilized split aptamer fragment to a fluorophore-tagged second fragment. Analyte binding modulates fluorophore-surface distance, switching between PEF enhancement (>15 nm) and quenching (<10 nm). Readout via surface plasmons on flat metal and localized surface plasmons on nanoparticle arrays will be studied for enhanced field intensity confinement to improve therapeutic drug monitoring.

Modelling of Charge Carrier Transport in Anisotropic Organic Semi-conductors

Basit A. and Toman P.

Abstract. We present a hybrid model for simulating charge carrier transport in anisotropic organic semiconductors, focusing on diketopyrrolopyrrole (DPP) derivatives. The model integrates a quantum mechanical description of charge carrier delocalization along linear molecular stacks, characterized by high charge transfer integrals, with semi-classical hopping between stacks in the remaining two dimensions. Key molecular parameters of the organic material will be obtained through a combination of molecular dynamics simulations and quantum chemical calculations. We will compare the predictions of our model with those of previous approaches. This molecular-scale model is designed to enhance the understanding and optimization of charge carrier mobility in organic field-effect transistors (OFETs).

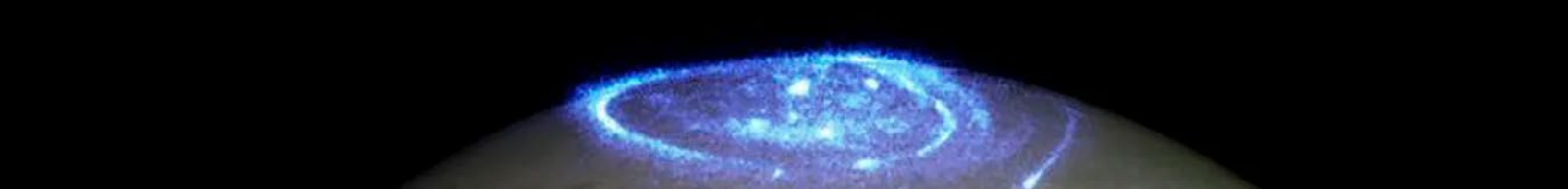

Tuning PEG Based Molecules for Cushioning Supported Lipid Bilayers Monitored by Graphene Induced Energy Transfer

Blanco-Campoy D. G., Sýkora J., López-Mora N., Volochanskyi O., Koeppe B. , Hof M., Kalbáč M., and Amaro M. M.

Abstract. In recent years, super-resolution microscopy techniques have undergone a great revolution in terms of spatial details. The enhance axial resolution is necessary for studying lipid bilayers, which are highly dynamic self-assembly with a typical thickness of about 5 nm. Graphene Induced Energy Transfer (GIET) is one of the approaches resolving axial distances of fluorescent emitters with nanometer resolution. This approach depends on graphene-induced fluorescence quenching, which reduces the lifetime in a distance-dependent manner. The GIET allows to discriminate between membrane organization in bottom and top leaflets. Our research aims to design and build substrates suited for GIET investigations on Supported Lipid Bilayers (SLBs). We use a graphene monolayer on a glass support that is coated with cushions made of Perylene-bisimide-Polyethylene Glycol (PBI-PEG) for this purpose. We have tested a number of PEG polymers with varying lengths and elaborating methods to achieve the best SLB formation. We use for SLB characterization fluorescence techniques and Atomic Force Microscopy (AFM) to confirm the correct SLB formation.

Electrochemical Evaluation of Antifouling Properties of Zwitterionic Polymer Brushes

Csiba M., Pilipenco A., Kolivoška V., and Vaisocherova-Lísalova H.

Abstract. Zwitterionic polymer brushes represent a class of surface coatings suitable for minimizing nonspecific adsorption. An electrochemical approach can be used to evaluate antifouling properties by monitoring changes in charge transfer resistance and redox probe permeability on the studied surface. To validate the electrochemical results, surface plasmon resonance can provide an independent and label-free monitoring of surface interactions. With this combined approach, we aim to obtain comprehensive understanding of the antifouling behavior of the polymer brush coatings.

Copper Nitride Nanoparticles Synthesized via Post-Magnetron Sputtering for Low-Temperature Hydrogen Sensing

Červenková V., Nikitin D., Cieslar M., Bajtošová L., Dopita M., Biederman H., Martinu L., and Choukourov A.

Abstract. Copper nitride (Cu_3N), a promising and defect-tolerant semiconductor, is gaining attention for catalysis and gas sensing. In this work, we present a sustainable, solvent-free method for synthesizing Cu_3N nanoparticles using reactive sputtering in nitrogen via a gas aggregation cluster source. The obtained 25 nm cubic NPs exhibit a semiconducting nature, thermal stability up to 175 °C and 300 °C in air and vacuum, respectively, and potential for mid-temperature hydrogen sensing applications.

Exciton–Exciton Annihilation in Ultrafast Spectroscopy

Charvatova K. and Maly P.

Abstract. Exciton–exciton-interaction two-dimensional spectroscopy (EEI-2DES) enables direct observation of exciton annihilation, with dynamics that reflect exciton diffusion through molecular complexes. By analyzing these signals, we can study energy transport even in nearly isoenergetic systems such as photosynthetic antennas. Our work extends the theoretical description of EEI-2DES to capture its spectral features. We aim to discover the possibilities of using this method to acquire deeper structural information about the sample from experimental data.

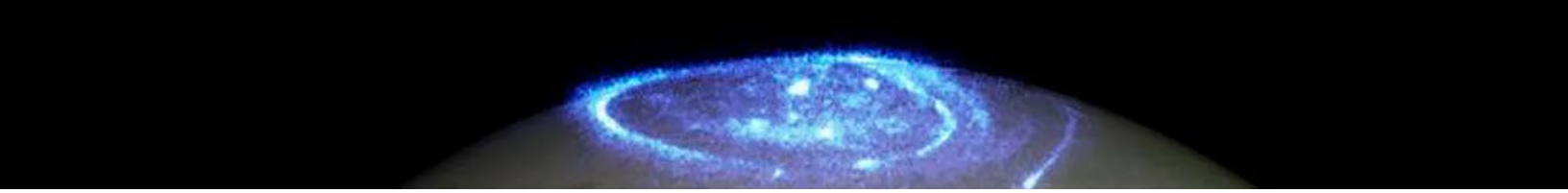

Substrate Binding in Enzyme Clusters: Effects of Crowders and Transient Interactions

Poolamanna A., Timr Š., Dašić M., and Hazrati M. K.

Abstract. In living cells, various enzymes have been found to assemble into transient structures that can appear and disassemble depending on external conditions. Such assemblies have been found in various pathways, including glycolysis, oxidative phosphorylation, purine synthesis, etc. However, the molecular mechanisms driving their formation and functional relevance remain poorly characterized. In this study, we develop a highly coarse-grained computational model based on insights from all-atom molecular dynamics simulations to investigate how the presence of crowders as well as transient interactions between enzyme assembly constituents—enzymes, substrates, and crowders—influence the active site occupancy. Our simulations allow us to identify the sets of conditions that lead to maximised or minimised substrate binding. These findings reveal how the properties of the crowded environment in enzyme assemblies govern the efficiency of metabolic pathways.

Exploring Resonance Raman Scattering and Stimulated Raman Scattering Effects in CrSBr

Sahu S., Palacios C. B., Juergensen S., Mosina K., Sofer Z., Velický M., Kusch P., and Frank O.

Abstract. CrSBr is an air-stable magnetic semiconductor and a van der Waals material with notable intrinsic properties, such as crystalline anisotropy, quasi-1D electronic behavior, and layer-dependent magnetism. In this talk, I will discuss the origin of the emission peak near 1.7 eV observed in its photoluminescence spectrum and the excitation energy-dependent Raman spectroscopy. I will also discuss the observation of stimulated Raman scattering (SRS) in CrSBr and CrSBrCl highlighting the interplay between electronic and vibrational states in CrSBr and the Raman gain, which surpasses those reported in many three-dimensional systems. Additionally, I will comment on the unusually high anti-Stokes to Stokes intensity ratio in CrSBr, which varies with laser power and crystal orientation. These findings underscore the unique vibrational and electronic interactions in these materials.

Crowders Alter Accessibility of Adenylate Kinase Conformational Space

Samanta M. ***and Timr S.***

Abstract. Enzymes in biological cells are surrounded by various biomolecules, unlike the isolated conditions in traditional in-vitro assays. These crowders can alter enzyme activity in a non-trivial way. Using all-atom molecular dynamics simulations, we studied the effects of different crowders on Adenylate Kinase. Crowders were found to interact closely with the enzyme, affecting its conformational changes and slowing domain fluctuations. These results show that cellular crowding can limit enzyme's accessibility to extreme conformations and influence enzyme function.

XUV Laser-induced Damage to Plasmid DNA at Temperatures Below and Above Freezing

Scheinpflug V., Burian T., Vysin L., Rocca J. J., Menoni C. S., and Juha L.

Abstract. The temperature dependence of radiation-chemical reactions can provide valuable insights into their underlying mechanisms. In this study, plasmid DNA samples were exposed to low-energy ionizing electromagnetic radiation at temperatures below freezing (−10°C) and at ambient temperature (20°C). Irradiation was carried out using a compact, table-top plasma-based source of coherent extreme ultraviolet (EUV) radiation. The EUV source is a capillary-discharge Ne-like Ar laser that emits nanosecond pulses at 46.9 nm. All irradiations were conducted in high vacuum, and sample temperature was controlled using Peltier thermoelectric modules. The results showed a pronounced temperature dependence in the yields of double-strand breaks (DSBs), whereas single-strand break (SSB) yields remained largely unaffected by temperature changes. The reduction in DSB yield at subzero temperatures supports the hypothesis that indirect effects—rather than direct, correlated strand interactions—are the dominant pathway for DSB induction. A high number of reactive species formed within the DNA's hydration shell are capable of reaching both strands to cause breaks.

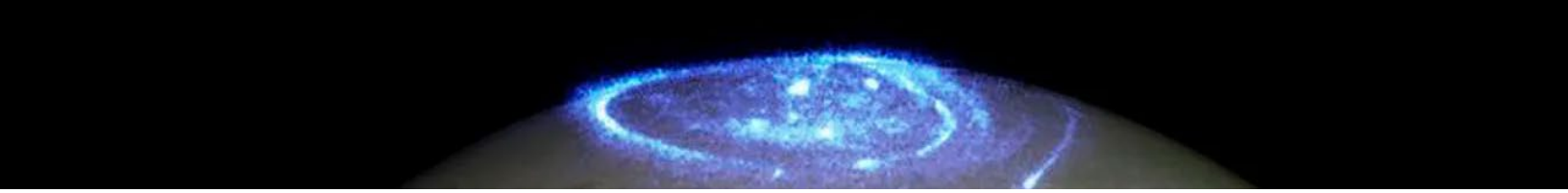

Gaussian Processes Enable Accurate and Efficient Free Energy Landscape Reconstruction

Skorna M., Janáčková Z., Yesylevskyy S., Shanks B., and Jungwirth P.

Abstract. Little known to the field of chemical physics, Gaussian Processes (GPs) and Bayesian inference offer a probabilistic framework for modeling complex chemical systems with rigorous uncertainty quantification. This talk introduces their theory and potential in atomistic modeling. Preliminary results on membrane–peptide and membrane–membrane interactions show how GPs provide accurate free energy surface reconstruction from sparse data and enable active learning, challenging traditional methods.

Gas Aggregation-based Synthesis of Functionalized Polymer Nanoparticles for Bioapplications

Skorvankova K., Solar P., and Krtous Z.

Abstract. A novel physical method for synthesizing polymer nanoparticles (NPs) is being developed using a gas aggregation source (GAS) with evaporation of a polymeric filament. Introducing Nitrogen into the GAS enables NPs functionalization. Functional groups may be used as binding sites for bioactive molecules, enabling applications in therapy, diagnostics and targeted drug delivery. The aim is to characterize the NPs, understand key dependencies, and tailor NPs for specific bioapplications.

F-5 PHYSICS OF SURFACES AND INTERFACES

In-situ Investigation of Anode Reaction in Anion Exchange Membrane Fuel Cell Using NAP-XPS

Chakraborty S.

Abstract. Understanding catalytic processes on the anode side in Anion Exchange Membrane Fuel Cells (AEMFCs) is critical for enhancing efficiency and durability. Despite being the best, the state-of-the-art fuel cell catalyst Platinum still shows sluggish reaction kinetics due to strong interaction with OH that blocks active sites for hydrogen needed to close the HOR (Hydrogen oxidation reaction). It has been shown that combining Pt with Ru improves the overall AEMFC efficiency. In this study, we perform studies on three different model catalyst surfaces i.e. Platinum (Pt), Ruthenium (Ru) and Platinum–Ruthenium (Pt–Ru) to understand the role of Ru. Using Near Ambient Pressure X-ray Photoelectron Spectroscopy (NAP XPS), we probe chemical and electronic changes at the model anode surface under water exposure. We showed that the Pt surface contains only one type of OH group strongly bonded to it. The addition of Ru results in the appearance of an additional OH peak that is related to the interaction with Ru and Pt. These types of OH seem to be less bonded to Pt and can effectively leave the surface for reaction, exposing free adsorption sites for hydrogen.

Stabilizing Platinum Oxygen Reduction Reaction Catalysts Through Rhodium Incorporation

Orság M., Mohandas Sandhya A. L., Skála T., Vorochta M., Briega-Martos V., Cherevko S., Matolínová I., and Khalakhan I.

Abstract. The limited long-term stability of cathode catalysts remains a barrier to widespread deployment of PEMFCs. Even platinum, a widely used ORR catalyst, is prone to degradation and dissolution in a fuel cell. To address this issue, Pt–Rh catalysts with varying Rh content were fabricated by magnetron sputtering and characterized using SEM, SRPES, CV and on-line ICP-MS. The results show that Rh incorporation enhances catalyst stability, reducing Pt dissolution under simulated operational conditions.

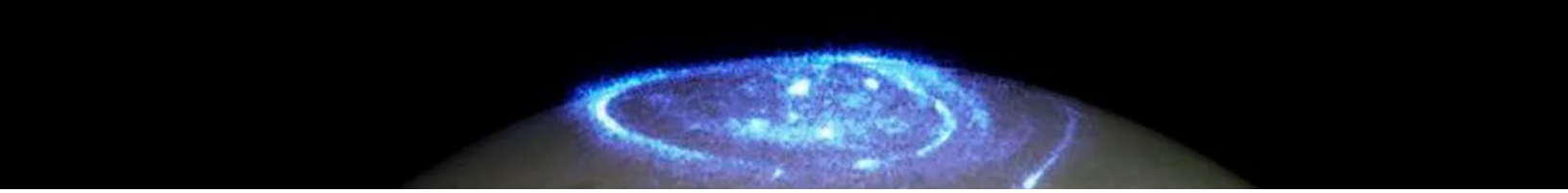

Charge Manipulation in Hematite Fe2O3 as a Route to Polaron Physics

***Sreekumar S.*, Caldentey L. A., Alexander A., Redondo J., Tobisch S., Kocan P., Riva M., and Setvin M.**

Abstract. The non-contact Atomic Force Microscopy (nc-AFM) technique has enabled breakthroughs in single-electron charge manipulation [1]. Here we use this capability to study polaron dynamics. Polarons are self-localized electrons or holes in ionic lattices that are crucial to material properties like conductivity, catalysis, and exotic phenomena such as high-temperature superconductivity and colossal magnetoresistance [2]. Polarons are studied in hematite Fe2O3 at the single quasiparticle limit, focusing on the fundamental mechanisms involved in their injection, formation, migration, and interaction with defects [3].

F-6 QUANTUM OPTICS AND OPTOELECTRONICS

Magneto-optical Spectroscopy of Materials with Structural Transformations

Makeš M., Zázvorka J., Hubert M., Veis M., and Heczko O.

Abstract. Magneto-optical spectroscopy is useful technique for spin-resolved electronic structure investigations. Regression analysis of ellipsometry data allows for a calculation of material properties, such as the relative permittivity tensor elements. To gain insight into the electronic structure of the material, computed permittivity tensor spectra can be either fitted to semiclassical theory predictions or compared to ab initio calculations. New findings on feromagnetic shape-memory alloy Ni-Mn-Ga in form of thin epitaxial films will be presented.

Ultrafast Spectroscopy of Single Light-Harvesting Complexes

Shein M., Malý P., and Garrow M.

Abstract. Ultrafast spectroscopy combined with single-molecule fluorescence enables probing of excitation dynamics in complex systems such as photosynthetic light-harvesting complexes. Time-resolved fluorescence microscopy enables tracking of excitation spectra, lifetimes, and transient changes at the single-complex level. This approach reveals dynamics obscured in ensemble measurements of heterogeneous systems. Initial findings show strong potential for uncovering key photophysical mechanisms.

Optically-induced Magnetic Dynamics in Altermagnetic Candidate MnTe

Střihavková J., Kimák J., Sadeghi Z., Kriegner D., Reichlová H., Springholz G., Schmoranzerová E., and Němec P.

Abstract. Altermagnets, materials with antiparallel ordering of magnetic moments and a spin-split electronic band structure, are promising candidates for spintronic applications. We have investigated magnetic dynamics of the thin-film altermagnetic candidate MnTe using time-resolved magnetooptics. In two regions of the sample, we observed the same quadratic magnetooptical effect but with different symmetry, indicating different orientations of the Néel vector in these regions.

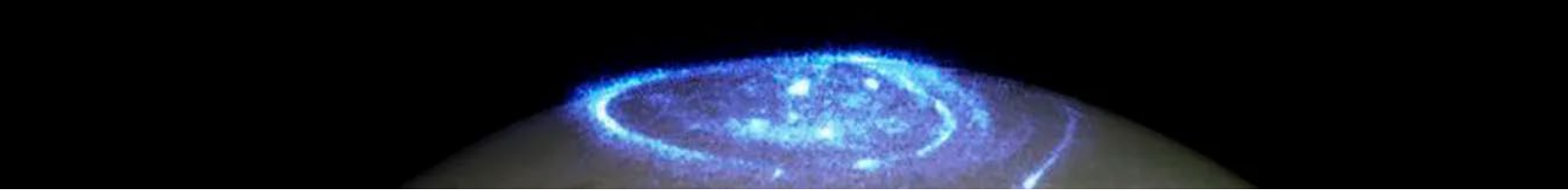

F-8 ATMOSPHERIC PHYSICS, METEOROLOGY AND CLIMATOLOGY

Application of Machine Learning to Severe Weather Prediction from Storm Top Indicators

Doležalová A., Seidl J., and Šťástka J.

Abstract. We present a case study using a machine learning model to detect overshooting tops (OTs) from visible satellite imagery and compare them with severe weather reports. The model successfully identified key convective areas, with varying levels of agreement across events. Some OTs aligned well with hail or wind reports, while others did not, showing the model's potential as a supportive but not definitive tool for severe weather assessment.

Orographic Gravity Waves and Their Representation in Models

Hajkova D.

Abstract. Orographic gravity waves are an important part of the atmospheric dynamics. They transport momentum from the surface to higher levels of the atmosphere. They exist on scales which are not fully resolved in global climate models and so they need to be parameterized. Parameterizations are created under set of many assumptions and are constrained by tunable parameters. We tested different components of the schemes to estimate their relevance and their dependence on the tuning of the parameters.

Utilization of Station Data for Statistical Processing of Model Tropospheric Ozone Concentrations in Europe

Peiker J., Karlický J., and Huszár P.

Abstract. Tropospheric ozone belongs among the most important pollutants and its concentrations are difficult to model, especially in future climate projections. To compensate for this uncertainty, statistical processing can be utilized by comparing a historic model run with observations and extrapolating the relationship to the projections. In this study, we introduce a method for postprocessing ozone concentrations which outperforms other methods from literature using European station data.

F-9 PARTICLE AND NUCLEAR PHYSICS

Study of Z-tagged Jet Structure in PbPb and pp Collisions at 5.36 TeV

Lelak E.

Abstract. The work explores jet production and their suppression in the quark–gluon plasma (QGP) formed in heavy-ion collisions at the LHC. By analyzing jet substructure and jets recoiling against Z boson, the study investigates how quarks and gluons lose energy while traversing the QGP. Data from the ATLAS experiment are used to probe medium-induced modifications of jets and deepen our understanding of this deconfined state of matter.

Reconstructing the Muon Production Depth Using Gradient Boosted Decision Trees

Östman L.

Abstract. Primary cosmic rays create cascades of particles when interacting with atmospheric nuclei. Muons with sufficient energy, produced in air showers, propagate to the ground. We present a method for reconstructing the atmospheric production depth of such muons using Boosted Decision Trees. A good reconstruction accuracy is found using simulated showers with zenith angles below 40 degrees and primary energies below 10^18 eV, appropriate for the underground muon detectors of the Pierre Auger Observatory.

Modern Amplitude Methods and Quantum Electrodynamics

Podivín D.

Abstract. In this work we apply the toolbox of modern amplitude methods to massless Quantum electrodynamics and related theories. We study maximum helicity violating amplitudes and show that they are fully determined by their soft behaviour and admit a simple factorized form in terms of soft factors and lower-point amplitudes. The formulae are recursively proven and their possible extensions are discussed.

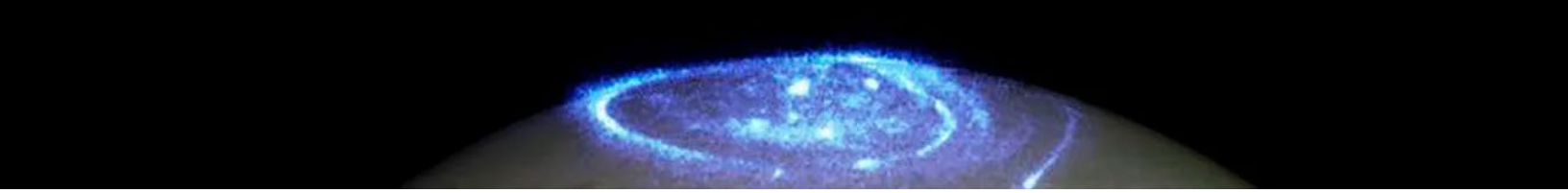

Implications of Baryon and Lepton Number Violation

Malinský M., Susič V., Gráf L., Gedeonová H., Plakkot V., and Starý D.

Abstract. Neutrino oscillations provide a clear signal of physics beyond the Standard Model. Proposed explanations, together with the baryon asymmetry of the Universe, suggest that baryon (B) and lepton (L) number may not be conserved. If B and L violation indeed occurs, rare processes such as proton decay or neutrinoless double-beta decay are allowed, making them promising probes of new physics. I will provide an overview of the key concepts and the state-of-art in the research of B and L violation.

The Hybrid Reconstruction of Showers Seen by the Pierre Auger Observatory

Syrokvaš K. and Novotný V.

Abstract. The Pierre Auger Observatory is dedicated to detecting and studying the highest-energy cosmic rays. By employing surface detectors (SD) and fluorescence telescopes (FD) in the so-called hybrid reconstruction, the Observatory estimates the properties of the primary particles that initiate cosmic-ray showers. Key properties include the energy, the depth of the shower maximum indicative of composition, and the arrival direction of the primary particles. We propose a modification of this hybrid reconstruction that has the potential to expand the dataset suitable for further analysis.

Forced Classifier Independence in General and Search for QCD Instantons in Particular

Vavricka R.

Abstract. QCD instantons remain an elusive missing piece of the standard model, a nonperturbative effect without any new particle associated, search thereof at the LHC by the ATLAS experiment will be described, along novel techniques from the realm of nebral networks.

F-12 PHYSICS EDUCATION AND GENERAL PROBLEMS OF PHYSICS

Translating the Force Concept Inventory in the Age of AI

Babayeva M., Dunlap J., and Widenhorn R.

Abstract. We present a study that translates the Force Concept Inventory (FCI) using GPT model. We assess the specific difficulties of translating a work in a scientific-focused topic using Large Language Models (LLMs). The FCI is a physics exam meant to evaluate outcomes of a student cohort before and after instruction in Newtonian physics. We examine the problem-solving ability of the LLM in both the translated document as well as the translation back into English and detail the language-dependent issues that complicate the translation. LLMs provide a new opportunity in expanding educational tools and assessments. At the same time, there are unique challenges and threats to the assessments. This case study will examine those opportunities, challenges and threats.

Critical Analysis of Thermodynamic and Statistical Physics Concepts in Highschool Textbooks and Electronic Materials

Blovský T.

Abstract. This contribution presents a critical analysis of high school textbooks on thermodynamics and molecular (statistical) physics, as well as selected educational websites. Emphasis is placed on the scientific accuracy of the introduced concepts and the interdisciplinary integration of the subject with other natural sciences (e.g., chemistry, biology). The analysis reveals that thermodynamic concepts are often introduced superficially, without connections to related scientific disciplines. Definitions are frequently incomplete or incorrect, which may contribute to student misconceptions. The statistical meaning of thermodynamic quantities (e.g., temperature) is generally omitted, and a clear conceptual link between thermodynamics and statistical physics is lacking.

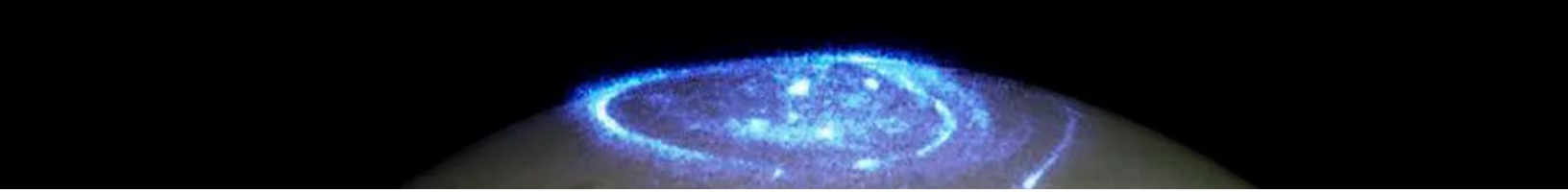

Differential Forms and Hodge Operator — Effective Mathematical Background for Physics

Bulušek P.

Abstract. Differential forms are a relatively common tool for both very economical writing of physics equations and for mathematical manipulations. In this paper we will show their use, together with the so-called Hodge operator, for effective transformations of differential operators into general coordinates. The paper belongs to the field of university physics education.

Why Pre-service Teachers Teach During Their Studies: Early Insights into Student–Teacher Experience

Cehakova L.* and *Chval M.

Abstract. The ongoing shortage of qualified physics teachers in Czechia has created opportunities for students enrolled in teacher education programmes to assume teaching positions. Several departments of teacher training have observed a growing number of physics education students engaging in teaching activities beyond their mandatory practice requirements — we call these students student-teachers. In this contribution we present the findings including motivations, experiences, and challenges faced by these student-teachers. A questionnaire survey was conducted in spring 2024 among 98 students enrolled in physics teacher training programmes at 9 Czech universities. We provide the study design and an analysis of the initial findings, focusing on student-teachers' motivations for entering the teaching profession and the workload they experience. The results indicate that financial necessity and the desire to gain practical teaching experience are the primary motivators to undertake teaching roles during studies. However, this dual role involves several risks, such as elevated stress levels.

University Training of Pre-service Teachers in Quantum Physics

Kafka J.

Abstract. With the rapid development of quantum technologies, it is essential for physics teachers to understand the basic principles of quantum physics. There are eleven university departments in the Czech Republic providing education programs for future physics teachers. This contribution presents a comparison of the syllabi related to quantum physics, atomic physics, and nuclear physics across these programs. To map and to compare the level of understanding of basic quantum principles among pre service teachers, the most suitable conceptual test was selected.

Teaching–Learning Sequence on Quantum Physics for High School Level — Design and Piloting

Legerská J.

Abstract. This contribution summarises preliminary results from piloting a teaching–learning sequence on quantum physics aimed at high school students. The sequence presents quantum physics in a conceptual way, with emphasis on its basic principles such as its probabilistic nature, principle of superposition, and quantum measurement. It takes into the account also high school teachers' perspectives on teaching this topic, which were investigated in our previous research.

Smart Devices and Digital Literacy in Physics Education

Nauš J.

Abstract. This contribution explores the integration of smart devices in physics education. It begins with a general discussion of the educational use of smartphones and tablets, highlighting both pedagogical benefits and common concerns. It then introduces key frameworks for understanding digital literacy (DigCompEdu, DiKOLAN). Practical use cases, such as Phyphox experiments, are presented, followed by a review of recent research on barriers to mobile device adoption in science teaching.

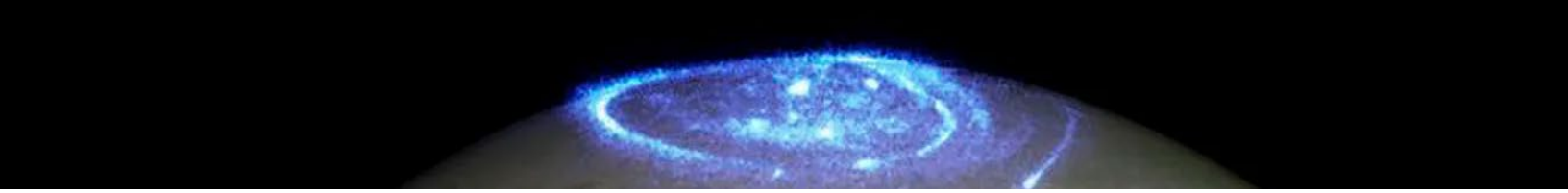

F-13 PHYSICS OF NANOSTRUCTURES AND NANOMATERIALS

Streptavidin Binging on Top of a DNA Origami Rectangle

Cardos K., Sala L., and Kocišek J.

Abstract. DNA Origami is a versatile nanotechnology technique that exploits the natural base-pairing of DNA to fold it into any desired two- or three-dimensional shape. One of the most relevant features of DNA Origami enables the precise nanoscale positioning of organic and inorganic materials. In this research work, we study the efficiency of binding streptavidin on the surface of a pre-designed rectangular DNA structure. By strategically modifying the sequence of specific strands, we arranged the streptavidin in a specific pattern and evaluated the molecular placement's efficiency, reproducibility, and fidelity.

Optimising Growth Parameters for 2D Transition-metal Dichalcogenides Using Chemical Vapour Deposition

Ghosh S., Varade V., and Vejpravová J.

Abstract. Despite many years of research on transition metal dichalcogenides (TMDs), achieving high-quality thin films through controlled synthesis remains challenging. Among the available methods, chemical vapour deposition (CVD) has emerged as a reliable approach to grow atomically thin layers. In this work, we optimise the CVD process by varying temperatures and gas flow rates. The technique is refined to produce wafer-scale thin films on SiO_2/Si substrates. Optical microscopy, AFM, Raman and Photoluminescence spectroscopy are used to characterise the as-grown TMD films.

MBE Growth of Mn-based Magnetic Materials

Kraus J., Křížek F., and Novák V.

Abstract. Magnetic materials with compensated atomic magnetic moments are a hot topic in today's spintronics. To prepare those materials in a quality applicable in spintronics, one needs to utilise a special growth technique — molecular beam epitaxy, which allows the growth of monocrystalline thin layers of materials with precisely controlled composition. This presentation intends to show MBE growth and properties of three Mn-based materials — antiferromagnetic Mn2As and CuMnAs and an altermagnetic candidate Mn5Si3.

Magnetotransport in Altermagnetic CrSb

Müller C., Wunderlich J., Reichlová H., Helm T., Thadatil S., Kotte T., Bommanaboyena S., Pospíšil J., Výborný K., Baj M., Scheffler D., and Kriegner D.

Abstract. Chromium Antimonide (CrSb) is due to its crystal symmetry and its compensated order classified as an altermagnet. CrSb exhibits sizeable spin splitting of 1.2 eV which is enabled by the non relativistic crystal field origin. We have available mm-sized CrSb single crystals grown by chemical vapour transport for which we have determined the crystal orientation via X-ray diffraction. Laboratory magnetotransport and magnetisation studies as well as preliminary pulsed field data,, obtained via a collaboration with HZDR are consistent with the compensated magnetic order and show indications of a multi-band transport behaviour.

Hexagonal Ferrites: Morphology, Texture and Properties

Spurná E.

Abstract. Hexagonal ferrites or in short hexaferrites are materials with unique multiferroic characteristics, that with a properly developed structure may result in magnetoelectric effect. A series of hexaferrite thin films was analyzed to determine the evolution of texture, morphology and magnetic characteristics. The sample series consisted of M-type hexaferrites with their bulk layer consisting of $SrFe_{12}O_{19}$ and seed layer of $SrFe_4Ga_8O_{19}$, grown on sapphire substrates cut in different orientations.